

IMPROVEMENT OF MODEL OF ALUMINIUM ALLOYS BEHAVIOUR FOR APPLICATION IN NUMERICAL SIMULATIONS OF WELDING

MOJMIR VANEK¹, JAROMIR MORAVEC², JAN RIHACEK¹

¹Brno University of Technology, Faculty of Mechanical Engineering, Institute of Manufacturing Technology Brno, Czech Republic

²Technical University of Liberec, Faculty of Mechanical Engineering, Department of Engineering Technology Liberec, Czech Republic

DOI : 10.17973/MMSJ.2016_11_2016124

e-mail : mojmir.vanek@vut.cz

This article describes how to modify numerical solutions to enable more accurate prediction of the size of heat affected zones (HAZ) during welding of heat treatable aluminium alloys. The size of HAZ affects properties of a weld joint, such as e.g. hardness and strength, and it is also a factor on residual stress and deformation after welding depends.

Welding experiments were performed using material EN AW-6082 to obtain input data for numerical simulations. Calibration thermo-metallurgical numerical analyses were performed using simulation software Sysweld, where data from the standard Sysweld material database were used. Subsequently, based on information from literature and data obtained during welding experiments, some changes of parameters in Leblonds formula (which describes metallurgical transformation in HAZ) were done.

The results obtained with modified material database show that it is possible to perform numerical simulations of aluminium welding with significantly more accurate prediction of the size of the HAZ.

KEYWORDS

numerical simulations, Sysweld, welding, aluminium alloys, heat affected zone, hardness

1 INTRODUCTION

Numerical simulations of welding and heat treatment are more and more used tool that allows to compare proposed technologies in terms of final properties of the weldment, deformation and risk of defects in welding. The widest usability is in areas where it is difficult to carry out an experiment for validation of the technology, or if the experiment cannot be done at all. In these areas any mistake could lead to significant economic losses. This can happen mainly in heavy industry and in energy sector, where numerical simulations are used e.g. to design technologies for welding of turbine rotors, their subsequent repair, welding of parts of steam generators, nuclear reactors etc.

Currently, there are approaches that allow numerical simulations of welding of various types of steel with very good results. But of course, numerical simulations have some

limitations. A typical example is welding of non-ferrous metals, e.g. aluminium alloys, where the current approaches do not lead to satisfactory accuracy. But simulations of welding of aluminium alloys are increasingly demanded by companies, mainly in the field of transportation sector and in aerospace industry.

The aim of this paper is to describe improving of numerical solutions which enable more accurate prediction of the size of the heat affected zone (HAZ) during welding of heat treatable aluminium alloys. The size of HAZ affects properties of a weld joint, such as e.g. hardness and strength and it is also an important input data for the mechanical part of numerical analyses, which determine the size of the residual stresses and deformation upon welding.

2 MATERIALS AND THEIR BEHAVIOUR DURING WELDING

The base material was heat treatable aluminium alloy EN AW-6082 in state T651 (after artificial aging) and filler material was welding wire ESAB OK Autrod 5087.

2.1 Base material

EN AW-6082 (AlSi1MgMn) is a widely used material, which finds its use e.g. in aircrafts and ground vehicles. According to TNI CEN ISO / TR 15608, the material is classified into group no. 23, subgroup no. 23.1. In Tab. 1, there is chemical composition of the alloy according to the standard EN 573.

Si	Mg	Mn	Fe	Cu
0.7 – 1.3	0.6 – 1.2	0.4 – 1.0	Max. 0.5	Max. 0.10
Cr	Zn	Ti	Other	Σ others
Max. 0.25	Max. 0.2	Max. 0.10	Max. 0.05	Max. 0.15

Table 1. Chemical composition of EN AW-6082 [%]

If aged Al-Mg-Si alloys are welded, there is a significant decrease of strength across the weld joint, as we can see in Fig. 1. Strength may fall up to the level of strength of annealed material. [Gitter 2008] [Michna 2005]

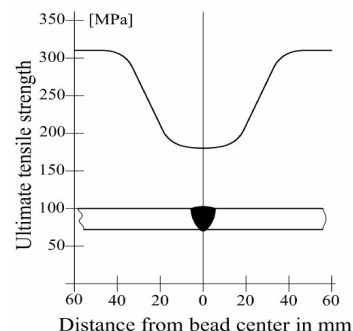


Figure 1. Evolution of ultimate tensile strength of EN AW-6082 in HAZ [Gitter 2008]

The explanation of such a behaviour is following: In areas of the weld, which were heated above the temperature of artificial aging, the volume of partially coherent precipitate increases and stable precipitates form. This phenomenon is known as overaging and is characterized by a decrease of mechanical properties. In areas that were heated above the solvus temperature, a process similar to dissolution annealing occurs - dissolution of precipitates. However, the process depends significantly on the temperature cycle in a particular point in the HAZ. [Ambriz 2015] [Kou 2003]

Material behaviour during heating can be derived from the diagrams called CHD (Continuous Heating Dissolution). This new type of diagrams of aluminium alloys was found and published by Osten. [Osten 2015] There is a CHD diagram of EN AW-6082 T6 in Fig. 2. The diagram describes stages of precipitation and dissolution of phases during heating from

20 °C to 600 °C for heating rates from 0.01 °C/s to 5 °C/s. In the diagrams we can see temperatures and times of the beginning of dissolution of Guinier-Preston zones (curve start B), dissolution of β (Mg_2Si) phase (start H), the beginning of precipitation of metastable phases such as β' α' (start d) and later their dissolution (start F). The curve labelled "end H" indicates the end of the dissolution of phase Mg_2Si and formation of the homogeneous solid solution.

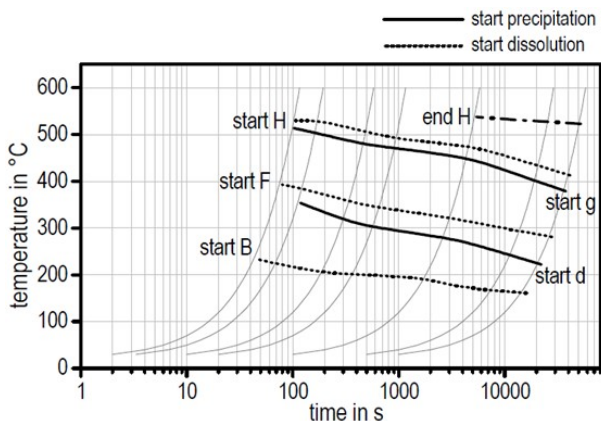


Figure 2. CHD diagram of EN AW-6082 T6 [Osten 2015]

2.2 Filler material

ESAB OK Autrod 5087 is an alloy AlMg4.5MnZr, which is used for welding of aluminium alloys containing up to 5 % Mg and alloys with higher strength. The material contains a slightly higher Zr content in order to improve the resistance against hot cracking of the weld metal. There is a chemical composition of the welding wire according to the producer in Tab. 2. There are typical mechanical properties of pure weld metal in Tab. 3. For welding experiments, commonly used wire diameter of 1.2 mm was chosen. [ESAB 2012]

Si	Mg	Mn	Zn	Zr
< 0.25	4.70	0.80	0.20	0.15

Table 2. Chemical composition of OK Autrod 5087 [%] [ESAB 2012]

Yield strength	Tensile strength	Elongation A_5	KV at 20 °C
130 MPa	280 MPa	30 %	35 J

Table 3. Mechanical properties of filler metal [ESAB 2012]

3 WELDING EXPERIMENTS

Welding experiments were performed at the workplace in Fig. 3. Components of the workplace is the fixture with line-type contact with the specimen, so it is possible to neglect simulation of heat transfer into the fixture and simulate only heat transfer into the still air.

Welding technology 131 (MIG) was selected, because this technology enables a relatively high degree of automation. This minimizes the effect of human faults on the welding process and in terms of computer simulation, is not necessary to consider e.g. variations in welding speed. To minimize other variables during welding of the experiment, it was decided that the welding will be done without preheating. Preheating increases the width of HAZ and in heat-treatable aluminium alloy it may cause so-called overaging, a drop of strength properties. For the experiment, a power source 550 BDH Puls Syn was used. Feed of the nozzle was provided by a linear device. Angle of the nozzle was 90° in the welding direction as well as in the direction perpendicular to the welding. The composition of the shielding gas was 70 % Ar and 25 % He.

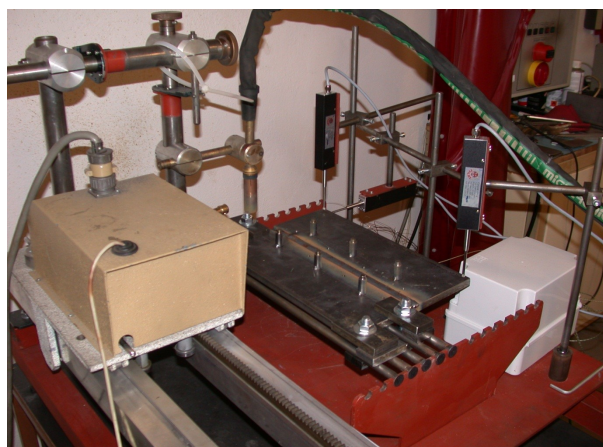


Figure 3. Workplace for welding experiments

Specimen for welding experiments with thickness 15 mm and dimensions 350 x 200 mm were mechanically cut from a metal sheet. A groove was milled into the specimens. The geometry of the groove is in Fig. 4. The angle of the groove is 60°, the bottom width of the groove is 1.5 mm, thus $A = 0.75$ mm, the dimension $B = 2$ mm and $W = 15$ mm. The geometry was selected in order to minimize unpredictable phenomena such as e.g. imprecise shape of tack welds and possible defects like lack of penetration or excess penetration of the weld deposit at the root side.

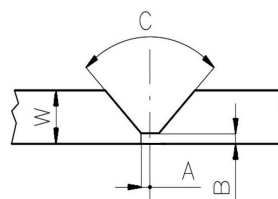


Figure 4. Geometry of the groove

During welding of the experiment, a three-pass weld was created. There are real welding parameters monitored during the process in Tab. 4.

Pass	I [A]	U [V]	Welding speed [$m \cdot min^{-1}$]
1 st	228.7	27.5	0.413
2 nd	241.8	28.2	0.375
3 rd	247.6	28.6	0.350

Table 4. Welding parameters

The length of the root pass was 350 mm, the length of the 2nd pass was 261 mm and length of the 3rd pass was 207 mm. This enabled to create macro-structures of each of the passes, then measure the dimensions of fusion zones. It was also possible to determine the influence of welding of next passes on the base material and filler material of the previous passes. There are dimensions of the passes and fusion zones for the finite element model and model of the heat sources in Tab. 5 and macro-structures in Fig. 5 and 6.

Pass	Area [mm^2]	Width [mm]	Penetration [mm]
1 st	41.6	9.6	3.9
2 nd	54.1	12.8	7.3
3 rd	73.9	16.2	7.2

Table 5. Dimensions of molten zones

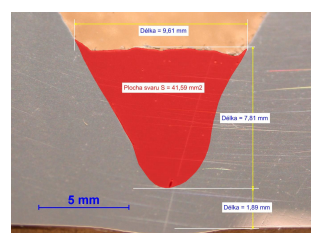


Figure 5. Molten zone of the 1st pass

5 CALIBRATION OF THE SIMULATION

Based on the experimental specimen, a computational model was created. The model consists of 149 074 elements and 132 314 nodes (see Fig. 8). However, the mesh was refined in areas of expected HAZ (see Fig. 9). Thermal boundary conditions were defined as heat transfer into the still air by convection and radiation.

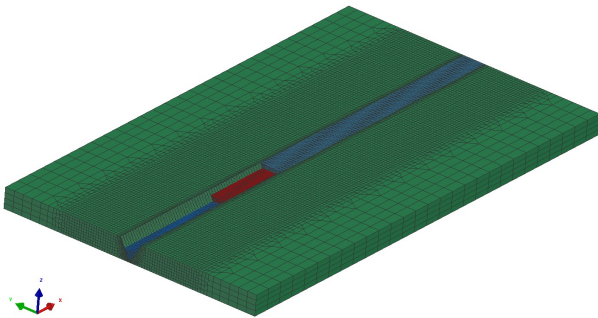


Figure 8. Computational model for finite element method

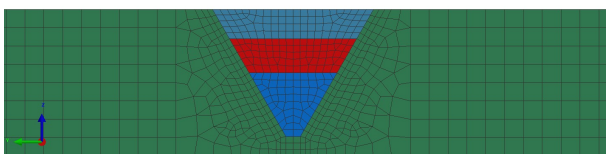


Figure 9. Detail of the finite element mesh in HAZ

It is necessary to realize the complexity of the welding process, because there is an interaction between number of different physical processes. In such a complex process, we cannot always precisely identify all the input parameters for the numerical analysis, such as e.g. exact value of heat transfer efficiency, or parameters a , b , c and d in formulas for definition of the heat source (1) and (2). Therefore, for calculations with the requirement of high accuracy, calibration numerical analyses are needed. The calibration involves performing of a simple welding experiment which is then simulated. The aim is a comparison of dimensions of fusion zones between the calculation and macro-sections of real welds performed during welding experiment. If the dimensions of the weld pool vary, input parameters for the simulation have to be corrected.

In Fig.10, there is temperature field and fusion zone during welding of the first pass as a result of the last calibration analysis. This was compared to the molten zone in Fig. 5.

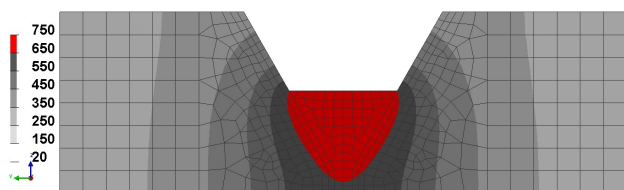


Figure 10. Temperature fields [°C] and molten zone during welding of the first pass in the cross-section

For the calibration analyses, materials from the standard material database of the Sysweld software were used. Properties of Al-Mg-Si were assigned to the base material and properties of Al-Mg-Mn to the filler material. After the models of heat sources were calibrated, heat-affected zones were displayed. As a result, contours of the initial phase the material (T651) were selected.

In the areas where the material was unaffected by heat, there is 100 % of the initial phase. In the contrary, in areas very close to the weld joint, there is 0 % of the initial phase. As boundaries of resolution, value of 2 % of the initial phase was chosen, because decrease of the initial phase of 2 % causes a decrease

in hardness of approximately 1 HV. This is evident from the results of hardness measurement in Fig. 7. So, the areas with more than 98 % of the initial phase are orange-coloured in Fig. 11 to 16, whereas the areas with less than 2 % of the initial phase are blue-coloured in Fig. 11 to 16. Therefore, blue and green colour in the following figures show HAZ, while the base material is orange-coloured.

Position of the blue-green interface corresponds to the location of the smallest hardness after welding of the particular pass. Distance of the smallest hardness from the axis of the weld is labelled as "E". Position of the green-orange interface corresponds to the location where the hardness of the base material is reached. Distance of this interface from the axis is labelled "G".

In Fig. 11, 12 and 13, there are results of metallurgical part of the numerical analysis using the old material model, it means model from the standard Sysweld material database. There are values of parameters P_{eq} and τ in formula (3) of this model in Tab. 6 and 7.

There is a contour-type result of the HAZ of the 1st pass in the cross-section in Fig. 11. Calculated value of E is 12.2 mm and calculated value of G is 23.3 mm.

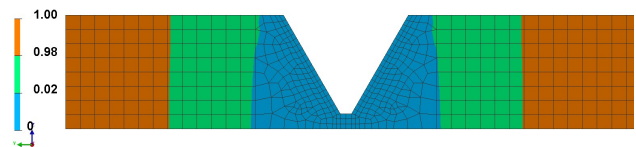


Figure 11. Distribution of initial phase [-] in HAZ after the 1st pass in the cross-section, old material model

There is a contour-type result of the HAZ of the 2nd pass in the cross-section in Fig. 12. For this pass, $E = 16.8$ mm and $G = 30.8$ mm.

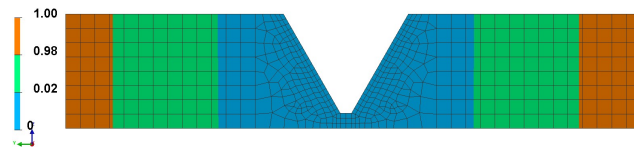


Figure 12. Distribution of initial phase [-] in HAZ after the 2nd pass in the cross-section, old material model

There is HAZ of the 3rd pass in the cross-section in Fig. 13. Calculated value of E is 18.0 mm and calculated value of G is 32.7 mm.

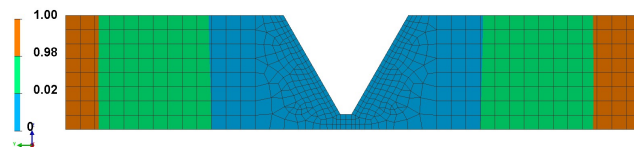


Figure 13. Distribution of initial phase [-] in HAZ after the 3rd pass in the cross-section, old material model

6 ESTIMATION OF PARAMETRES

If we compare measured values to values calculated using the old material database, we can see that the results do not correspond well. Obviously, the old material model needs some improvements.

A temperature range, where the phase transformation according to the old model occurs, can be identified from the Tab. 6. It starts at the temperature of 200 °C and material heated over 300 °C was fully transformed from the initial phase to the phase with low mechanical properties. On the other hand, from the CHD diagram in Fig. 2, dissolution of Guinier-Preston zones in EN AW-6082 starts at 170 °C for the slowest

heating rate. Of course, for higher heating rates it starts at higher temperatures, but from the nature of equation (3), the parameter P_{eq} is not a function of the heating rate. Similarly, the end of dissolution of phase Mg_2Si can be identified: The formation of the homogeneous solid solution is finished at 520 °C. According to the findings, we can transform Tab. 6 to Tab. 8 and change values of the parameter P_{eq} in the material database.

Temperature [°C]	P_{eq} [-]
170	0
520	1

Table 8 Values of parameter P_{eq} in formula (3) for material EN AW-6082

7 VERIFICATION OF THE MODEL

Thermo-metallurgical analysis with improved material database was carried out. All input parameters were exactly same as in the final calibration analysis described in chapter 5, except values of parameter P_{eq} in the metallurgical model. Values in Tab. 8 were used instead the values in Tab. 6. There are metallurgical results of this analysis in the following figures.

There is contour-type result of the HAZ of the 1st pass in the cross-section in Fig. 14. Position of the blue-green interface shows the location of the smallest hardness. Position of the green-orange interface shows the place, where the hardness of the base material is reached. Calculated distance of the smallest hardness from the axis is $E = 6.2$ mm and calculated distance where the hardness of the base material is reached is $G = 24.0$ mm.

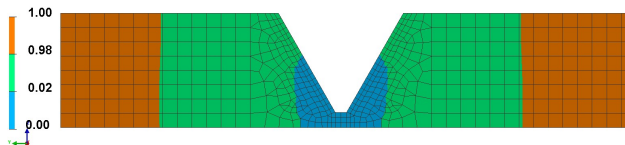


Figure 14. Distribution of initial phase [-] in HAZ after the 1st pass in the cross-section, new material model

There is HAZ of the 2nd pass in the cross-section in Fig. 15. Calculated value of E is 7.5 mm and $G = 32.1$ mm.

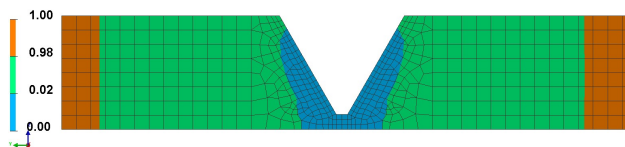


Figure 15. Distribution of initial phase [-] in HAZ after the 2nd pass in the cross-section, new material model

There is HAZ of the 3rd pass in Fig. 16, $E = 7.5$ mm and $G = 34.3$ mm.

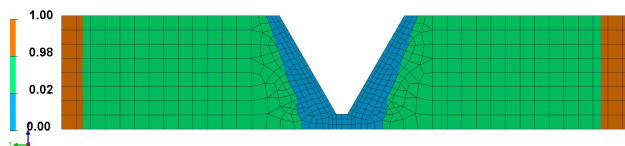


Figure 16. Distribution of initial phase [-] in HAZ after the 3rd pass in the cross-section, new material model

8 DISCUSSION OF THE RESULTS

There is a comparison of calculated and measured values of mentioned distances in Tab. 9. Calculated distances of the smallest hardness from the axis are in rows "E" and calculated distances where the hardness of the base material is reached are in row "F". There are measured values in the column "Experiment" and calculated values for the old and the new database in the next two columns.

Pass	Length	Experiment	Simulation	
			Old model	New model
1 st	E	6.5	12.2	6.2
	G	30.0	23.3	24.0
2 nd	E	8.0	16.8	7.5
	G	31.5	30.8	32.1
3 rd	E	8.0	18.0	7.5
	G	43.0	32.7	34.3

Table 9. Values of E and G, distance from the axis of the weld [mm]

Using the new model, there is highly increased accuracy for estimation of value E, but the prediction of G was improved gently. We can expect that further refinement can be reached by estimation of parameter τ (which involves time delay) and function $f(\dot{T})$, which involves heating rate. This will be the aim of further research.

9 CONCLUSIONS

The article described how to modify metallurgical model to enable more accurate prediction of the size of heat affected zones during welding of aluminium alloys EN AW-6082 T6.

Welding experiments were carried out to obtain input data for numerical simulations. Calibration thermo-metallurgical numerical analyses were performed using simulation software Sysweld, where data from the standard Sysweld material database were used. Subsequently, based on Continuous Heating Dissolution (CHD) diagram, some changes of parameter P_{eq} in Leblonds formula (which describes metallurgical transformation in HAZ) were done.

The results obtained with modified material database show that it is possible to perform numerical simulations of aluminium welding with significantly more accurate prediction of the size of the HAZ.

REFERENCES

- [Ambriz 2015] Ambriz, R.R. and Jarmillo, D. Mechanical Behavior of Precipitation Hardened Aluminum Alloys Welds. In: W.A. Monteiro, ed. Light Metal Alloys Applications [online]. InTech, 2014, pp 35-59 [cit. 2016-06-18]. Available from <<http://www.intechopen.com/books/light-metal-alloys-applications>>. ISBN 978-953-51-1588-5.
- [ESAB 2012] Catalogue of Filler Metals for Welding. Vamberk: ESAB Vamberk, s.r.o., 2012. (in Czech)
- [ESI 2016] ESI GROUP. SYSWELD 2016: Reference Manual. 2016
- [Furrer 2010] Furrer, D.U. and Semiatin, S.L. ASM Handbook, Volume 22B: Metals Process Simulation. Materials Park, OH, USA: ASM International, 2010. ISBN 1-61503-005-0
- [Gitter 2008] Gitter, R. Design of Aluminium Structures: Selection of Structural Alloys. 32 p. In: Workshop EUROCODES – Background and Applications – Session EN 1999-Eurocode 9: Design of Aluminium Structures, Brussels, 2008.
- [Kik 2015] Kik, T. et al. Numerical Analysis of Residual Stresses and Distortions in Aluminium Alloy Welded Joints. Applied Mechanics and Materials. Switzerland: Trans Tech Publications, 2015, Vol. 809-810, pp 443-448. ISSN 1662-7482
- [Kou 2003] Kou, S. Welding Metallurgy. Hoboken, NJ, USA: John Wiley & Sons, 2003. ISBN 0-471-43491-4

[Michna 2005] Michna, S. et al. Encyclopaedia of Aluminium. Decin: Alcan Decin Extrusions, 2005. ISBN 80-890-4188-4 (in Czech)

[Osten 2015] Ossten, J. et al. Dissolution and Precipitation Behaviour During Continuous Heating of Al-Mg-Si Alloys in a Wide Range of Heating Rates. Materials, 2015, 8(5), pp 2830-2848. ISSN 1996-1944

CONTACTS

Ing. Mojmir Vanek
Brno University of Technology
Faculty of Mechanical Engineering
Institute of Manufacturing Technology
Technicka 2896/2, 616 69 Brno, Czech Republic
e-mail: mojmir.vanek@vut.cz